

1 **Identification of genomic regions affecting production traits**

2 **in pigs divergently selected for feed efficiency**

3 Emilie Delpuech¹, Amir Aliakbari¹, Yann Labrune¹, Katia Fève¹, Yvon Billon², Hélène
4 Gilbert¹, Juliette Riquet^{1*}

5 ¹GenPhySE, Université de Toulouse, INRAE, F-31326 Castanet-Tolosan, France

6 ²GenESI, INRAE, F-17700 Surgères, France

7

8 *Corresponding author

9

10 Email addresses:

11 ED: emilie.delpuech@inrae.fr

12 AA: amir.aliakbari@inrae.fr

13 YL: yann.labrune@inrae.fr

14 KF: katia.feve@inrae.fr

15 YB: yvon.billon@inrae.fr

16 HG: helene.gilbert@inrae.fr

17 JR: juliette.riquet@inrae.fr

18

19

20

21

22

23 **Abstract**

24 **Background**

25 Feed efficiency is a major driver of the sustainability of pig production systems. Understanding
26 biological mechanisms underlying these agronomic traits is an important issue whether for
27 environment and farms economy. This study aimed at identifying genomic regions affecting
28 residual feed intake (RFI) and other production traits in two pig lines divergently selected for
29 RFI during 9 generations (LRFI, low RFI; HRFI, high RFI).

30 **Results**

31 We built a whole dataset of 570,447 single nucleotide polymorphisms (SNPs) in 2,426 pigs
32 with records for 24 production traits after both imputation and prediction of genotypes using
33 pedigree information. Genome-wide association studies (GWAS) were performed including
34 both lines (Global-GWAS) or each line independently (LRFI-GWAS and HRFI-GWAS). A
35 total of 54 chromosomic regions were detected with the Global-GWAS, whereas 37 and 61
36 regions were detected in LRFI-GWAS and HRFI-GWAS, respectively. Among those, only 15
37 regions were shared between at least two analyses, and only one was common between the three
38 GWAS but affecting different traits. Among the 12 QTL detected for RFI, some were close to
39 QTL detected for meat quality traits and 9 pinpointed novel genomic regions for some harbored
40 candidate genes involved in cell proliferation and differentiation processes of gastrointestinal
41 tissues or lipid metabolism-related signaling pathways. Detection of mostly different QTL
42 regions between the three designs suggests the strong impact of the dataset on the detection
43 power, which could be due to the changes of allelic frequencies during the line selection.

44 **Conclusions**

45 Besides efficiently detecting known and new QTL regions for feed efficiency, the combination
46 of GWAS carried out per line or simultaneously using all individuals highlighted the
47 identification of chromosomic regions under selection that affect various production traits.

48

49 **Background**

50 Feed efficiency is a major driver of the sustainability of pig production systems. It represents
51 from 50 to 83 % of cost productions depending on the countries and systems [1]. The feed
52 efficiency is also a principal lever to reduce the environmental footprints of the production [2].
53 The cost of feeding in pig production is usually measured by the computation of feed conversion
54 ratio (FCR). Indeed, FCR is a ratio between two traits of interest for most breeding schemes
55 (feed intake and growth rate), and incorporating it in selection indexes makes it difficult to
56 accurately anticipate responses to selection on this trait and the correlated traits [3]. In 1963,
57 Koch et al. [4] proposed residual feed intake (RFI) as an alternative to quantify feed efficiency,
58 to overcome the limits of FCR. The RFI is the difference between individual feed intakes and
59 predicted feed intake for the animal maintenance and production requirements. It is generally
60 computed as a multiple linear regression of daily feed intake on production traits (growth rate
61 and body composition traits in growing animals), and on the average metabolic body weight of
62 the animal during the period, as an indicator of maintenance requirements. As a result, selection
63 for RFI generates limited correlated responses on the other production traits, as shown in several
64 selection experiments in pigs [5, 6], and other species [7]. However, accurate individual feed
65 intake recording for pigs raised in groups is costly, and large efforts are devoted to facilitate the
66 improvement of feed efficiency, by either identifying biomarkers [8, 9] or genomic markers
67 (for instance [10, 11]). Despite these efforts, the difficulty to find quantitative trait loci (QTL)
68 or genomic variant affecting feed efficiency related traits translates in the PigQTLDB statistics
69 [12]: only 394 QTL are listed for feed conversion type of traits, and 350 for feed intake type of
70 traits, whereas more than 2,000 are reported for growth traits, and more than 3,200 for fatness
71 traits (PigQTLDB, access Sept 2020, [https://www.animalgenome.org/cgi-](https://www.animalgenome.org/cgi-bin/QTLdb/SS/index)
72 [bin/QTLdb/SS/index](https://www.animalgenome.org/cgi-bin/QTLdb/SS/index)). Genomic information acquired in established divergent lines for the trait

73 of interest can be used to increase the power of detection of genomic variants for lowly heritable
74 or highly polygenic traits, as RFI in pigs [10] and litter traits in rabbits [13].

75 In this study, we aimed at identifying genomic regions affecting RFI and other
76 production traits in two pig lines divergently selected for RFI during 9 generations [5], by
77 combining an extensive genotyping of all breeding animals of the lines, and the extensive
78 phenotyping of their progeny. GWAS were applied to growth, feed intake and feed efficiency,
79 carcass composition and meat quality traits on the full dataset. Different subsets of the
80 population were used to suggest biological hypotheses for the genetic background of the traits
81 in the two divergent lines, and decipher whether the chromosomal regions affecting RFI
82 differed between lines.

83 **Methods**

84 **Ethic statement**

85 All pigs were reared in compliance with national regulations and according to procedures
86 approved by the French Veterinary Services at INRA experimental facilities. The care and use
87 of pigs were performed following the guidelines edited by the French Ministries of High
88 Education, Research and Innovation, and of Agriculture and Food
89 (<http://ethique.ipbs.fr/sdv/charteexpeanimale.pdf>).

90 **Design**

91 The data were obtained from a divergent selection experiment on RFI carried out at the INRA
92 experimental units GenESI since 2000 (Surgères, France,
93 <https://doi.org/10.15454/1.5572415481185847E12>), on growing pigs from the French Large-
94 White (LW) population. The selection procedures were described by Gilbert et al. [5]. In brief,
95 the lines were established from 30 matings of LW animals (F0). From these litters, 116 males
96 were tested to select the 6 most efficient (LRFI) and 6 least efficient (HRFI) males as founders
97 of two divergent lines, and about 40 pairs of sibs were randomly assigned to each line. In the

98 following generations, from G1 to G9, 96 males from each line were tested for RFI to select 6
99 extreme low or high boars depending on the line. In addition, 35 to 40 females were randomly
100 chosen within-line in each generation to produce the next generation. No selection was applied
101 for females. From G1, matings were organized for at least two successive litters. Until G5, the
102 first litter provided boars candidates for selection and future breeding females, and castrated
103 males and females from the second parity were tested to evaluate the direct and correlated
104 responses to selection on major production traits, including carcass composition and meat
105 quality traits. After G5, selection was applied to parity 4 or 5, and responses to selection were
106 measured on pigs born in parity 2 and 3. Hereafter, the breeding animals will be called
107 “breeders” and animals tested for responses to selection will be called “response animals”.

108 **Phenotypes**

109 In each generation, 48 females and 48 castrated males per line were produced as response
110 animals, and tested individually during the growing-finishing period (~28 kg to ~107 kg) for
111 body weight (BW0 at the start of the test and BW1 before slaughter) and daily feed intake (DFI)
112 using a single-place electronic feeder (ACEMA 64; Skiold Acemo, Pontivy, France) to compute
113 average daily gain (ADG) and feed conversion ratio (FCR) during the test period. The dressing
114 percentage (DP) was computed based on weight records of warm carcass at slaughter. Twenty
115 four hours after slaughter, backfat thickness measured on carcass (carcBFT), and the weights
116 of ham (Ham_W), loin (Loin_W), belly (Belly_W), shoulder (Shoulder_W), and backfat
117 (BF_W), following a standardized cut, were recorded on the cold half carcass. The lean meat
118 content (LMCcalc) was evaluated according to the method of Daumas [14]. Meat quality
119 measurements included pH on *adductor femoris* muscle (AD), *semimembranosus* muscle (SM),
120 *gluteus superficialis* muscle (GS), and *longissimus dorsi* muscle (LM), colorimetry L*, a* and
121 b* on GS and *gluteus medius* muscle (GM), and water-holding capacity (WHC) assessed on
122 GS according to the procedure described by Charpentier et al. [15]. Finally, meat quality index

123 (MQI) was calculated from measurements of pH in SM, L* on GS and WHC according to the
124 model proposed by Tribout et al. [16]. RFI was defined as the residual of a multiple linear
125 regression as follows: $RFI = DFI - (1.48 \times ADG) + (23.2 \times LMC_{calc}) - (99.1 \times AMBW)$,
126 where AMBW is the average metabolic body weight during the test period and is equal to
127 $(BW1^{1.6} - BW0^{1.6}) / [1.6 (BW1 - BW0)]$ [17]. Contemporary group, gender and pen size were
128 added as fixed effects in the model, as described by Gilbert et al.[5].

129 **Genotyping**

130 Genomic DNA was purified from individual biological samples of the sires and dams of all
131 generations using standard protocols. Over time, two different Illumina medium density SNPs
132 chips were used according to the genotyping protocols defined by the supplier (at Technological
133 Center, Genomics and Transcriptomics Platform, CRCT Toulouse). First batch comprising 286
134 animals was genotyped for 64,232 SNPs using the Porcine SNP60v2 BeadChip (60K SNPs
135 chip), and a second batch of 1,356 animals was genotyped using the Porcine HD Array GGP
136 chip comprising 68,516 SNPs (70K SNPs chip). Genotypes were obtained using the Genome
137 Studio software (V2.0.4) and coded as 0, 1 and 2 corresponding, respectively, to individuals
138 homozygous for the minor allele, heterozygous and homozygous for the major allele. In
139 addition, 32 G0 founders (12 G0 sires, and 20 G0 dams that had most contribution to the
140 subsequent generations) were genotyped with the Affymetrix Axiom Porcine HD Genotyping
141 Array chip (Gentyane Plateform, UMR 1095 INRAE Clermont-Ferrand) consisting of 658,692
142 SNPs (650K SNPs chip).

143 For each SNPs panel, quality control was performed using PLINK software (V1.90)
144 [18]: SNPs with a call frequency (CF) < 95% and a minor allele frequency (MAF) < 1% were
145 excluded, and animals with a call rate (CR) < 90% were discarded. Unmapped SNPs and SNPs
146 located on sex chromosomes were removed following the Sscrofa11.1 assembly of the
147 reference genome (https://www.ensembl.org/Sus_scrofa/Info/Index)[19].

148 **Genotypes imputation**

149 Two successive imputations were performed using the FImpute software [20]. A first level of
150 imputation was performed with markers of 60K and 70K SNPs chips, based on 29,957 SNPs in
151 common, to homogenize the medium density genotyping data available for the 1,632 breeders
152 of the lines. This leads to an intermediate dataset of 66,988 SNPs imputed from both medium
153 density (MD) chips (60K and 70K SNPs chips). In a second step, the genotypes of the high
154 density (HD) SNPs chip were imputed for all breeders using the HD SNPs genotypes of the 32
155 G0 founders. A set of 45,708 SNPs was in common between MD imputed genotypes and HD
156 SNPs chip. A total of 570,447 SNPs distributed over the 18 pig autosomes, was finally available
157 for 1,632 breeding animals.

158 To evaluate the imputation accuracy, first, five successive batches of 1,000 SNPs were
159 randomly selected among the common SNPs in the 60K and 70K SNPs chips. For each SNPs
160 batch, the genotypes of these SNPs were set as missing for all animals genotyped with the 60K
161 SNPs chip and imputed from the 70K SNPs chip information. Therefore, a total of 5,000 SNPs
162 with real and imputed genotypes were used to compute Pearson correlations for each of the 286
163 pigs with 60K genotypes. Similarly, five batches of 1,000 SNPs were randomly selected from
164 common markers of both MD SNPs chips, animals genotyped with the 70K SNPs support were
165 re-coded as missing, and Pearson correlations between true and imputed genotypes were
166 computed for the 1,346 animals with 70K SNPs genotypes. Then, to evaluate the imputation
167 quality to the HD, the same strategy of removing successively five batches of 1,000 SNPs from
168 the data was applied using SNPs in common to the three chips. In addition, a leave-one-out
169 approach was applied to the 32 individuals with HD genotypes to evaluate the imputation
170 accuracy.

171 In addition, a multi-dimensional scaling (MDS) analysis was performed using R
172 software (V.3.6.2, R Core Team 2019) based on a identity-by-state matrix constructed with the
173 PLINK software [21].

174 **Predicted genotypes in response animals**

175 Response animals did not have genotypes themselves. An average expected genotypes of their
176 parents was computed for each animal from the imputed 650K genotypes. For each marker,
177 each individual was given the average genotype of the parents (0, 0.5, 1, 1.5 or 2), so within a
178 litter, all animals were assigned the same genotypes. Depending on the genotypic class, the
179 obtained genotype was, therefore, an approximation of the real genotype: (i) genotypes 0 and 2
180 were certain, as they resulted from two homozygous parents for the same allele ($0 \times 0 \rightarrow 0$ and
181 $2 \times 2 \rightarrow 2$), (ii) genotypes 0.5 and 1.5 included combinations of a homozygous genotype for one
182 allele and a heterozygous genotype ($0 \times 1 \rightarrow 0$ or 1 and $1 \times 2 \rightarrow 1$ or 2), and (iii) genotype 1 was
183 the most heterogeneous class, with a mixture of true genotypes ($0 \times 2 \rightarrow 1$) and uncertain
184 genotypes ($1 \times 1 \rightarrow 0$ or 1 or 2). Animals with a parent with a missing genotype were excluded
185 from the analysis.

186 **Genome-Wide Association Studies**

187 GWAS analyses were performed using GEMMA software (version 0.97) [22] on response
188 animals with their own phenotypes and their average genotypes from parents. Phenotypes were
189 adjusted for significant fixed effects and covariates (pen size, herd, sex, and contemporary
190 groups for *in vivo* measurements, slaughter date as fixed effects, and slaughter age as covariate
191 for traits recorded at the abattoir, and slaughter BW as covariate for carcBFT) using linear
192 models as proposed in Aliakbari et al. [23]. The resulting residues were integrated as
193 phenotypes in GEMMA. To account for the structure of the population in the GWAS analyses,
194 a pedigree relationship matrix **A** was computed. Association analyses were performed on the
195 24 traits available for 2,426 response animals.

196 The statistical model used to test one marker at a time was $\mathbf{y} = \mathbf{x}\beta + \mathbf{u} + \boldsymbol{\varepsilon}$, where \mathbf{y} is
197 the vector of adjusted phenotypes for all individuals; \mathbf{x} is a vector of genotypes at the tested
198 marker; β is the effect of the tested marker; \mathbf{u} is a vector of random additive genetic effects
199 distributed according to $N(0, \mathbf{A}\lambda\tau^{-1})$, with λ the ratio of the additive genetic variance and the
200 residual variance τ^{-1} ; $\boldsymbol{\varepsilon}$ is a vector of residuals $N(0, \mathbf{I}\tau^{-1})$, with \mathbf{I} the identity matrix. In
201 GEMMA, an efficient exact algorithm is implemented to first estimate λ , and next derive $\hat{\beta}$
202 and $\hat{\tau}$ for each marker [24].

203 The distributions of the p -values for the GWAS of each trait were checked using
204 quantile-quantile plots (Q-Q plot) and computing regression coefficients of the $-\log_{10}(\text{observed}$
205 p -values) on the $-\log_{10}(\text{expected } p\text{-values under } H_0)$. Inflation factors were lower than 1.23 for
206 all analyses, indicating low deviations from the distribution of the test statistic under H_0 . A
207 correction factor was anyway applied to all analyses to control type-I errors, by dividing each
208 p -value by the corresponding inflation factor to avoid the impact of this low deviation.

209 To account for the nominative type-I error and multiple testing issue, the significance
210 threshold was obtained after a Bonferroni correction as follows:

$$211 \quad -\log_{10}\left(\frac{0.05}{\sum(\text{number of independent tests/chromosome})}\right),$$

212 where number of independent tests was computed per chromosome as the number of principal
213 components required to describe 99.5% of the genotypic variability of each chromosome, after
214 a principal component analysis applied to the correlation matrix between genotypes of the SNPs
215 of the considered chromosome (square root (r^2) of linkage disequilibrium (LD) between each
216 pair of SNPs), as recommended by Gao et al. [25]. The chromosome-wide thresholds obtained
217 were between 3.09 and 3.16, thus a threshold of 3 was used to identify suggestive associations.
218 To determine genome-wide significance thresholds, the number of independent tests for the 18
219 autosomes was summed to apply a correction at the genome level. This threshold (4.5) was used
220 to identify significant associations.

221 Three types of populations were considered for GWAS. First, the full dataset combining
222 the two lines was analyzed in a global analysis (thereafter called Global-GWAS). Then, to
223 evaluate if some QTL were segregating in one line only, the analyses were repeated within line
224 (thereafter called Lines-GWAS, or HRFI-GWAS and LRFI-GWAS when only one line was
225 referred to).

226 To define QTL intervals, for each combination of population and trait, the genome was
227 divided into 1 Mb windows following the Sscrofa11.1 assembly of the reference genome. The
228 1 Mb windows with at least one SNP with significant p -value at 5% genome-wide ($-\log_{10}(p$ -
229 $value) \geq 4.5$) were retained, and adjacent windows with significant signals were combined into
230 a single QTL window per trait. In a second step, the adjacent and overlapping significant
231 windows between traits were combined using the same approach as presented above, thus
232 allowing a complete list of QTL regions to be subsequently analyzed. When a QTL region was
233 significant for several traits, for each of them, the most significant marker and the associated
234 allelic substitution effect was retained to tag the QTL (trait x region) for this trait in further
235 analyses – thereafter called SNP-QTL.

236 The QTL positions were compared to previously mapped QTL in pigs using the
237 pigQTLdb database [12], and QTL significant for RFI trait were screened for functional
238 candidate genes using Ensembl annotation V.101 (August 2020).

239 **Changes of allelic frequencies of SNP-QTL**

240 The power of detection in GWAS is strongly influenced by the allelic frequencies of the
241 analyzed markers [26]. Within each QTL window, the most significant SNP was considered to
242 examine the changes of allele frequencies with line selection. These SNP-QTL allele
243 frequencies were estimated for the response animal genotypes, i.e. from their average
244 genotypes. To find out how selection affected allele frequencies, and thus power of detection,
245 allele frequencies were computed by adding animals from one generation at a time, starting

246 from G1 individuals alone. Then, the allele frequencies adding G2 response animals were
247 obtained by combining genotypes of G1 and G2 response animals, and so on until G9. The
248 estimated frequencies in G9 (using all the animals from G1 to G9) corresponded to the
249 informativeness of the markers used in the main GWAS by line. A regression of the generation
250 (1 to 9) on the SNP allele frequencies was then applied to test changes of allelic frequencies on
251 cumulative datasets over generations. For each SNP-QTL, the significance of the slope was
252 estimated in each line using a Wald test. An average evolution score was compute for each QTL
253 region ($9 \text{ generations} * (|\text{slope}_{\text{HRFI}}| + |\text{slope}_{\text{LRFI}}|)$) when the slope value was different from zero
254 with $p < 0.05$. To reflect the evolution per trait, an average value over all the QTL regions
255 detected for each trait was computed.

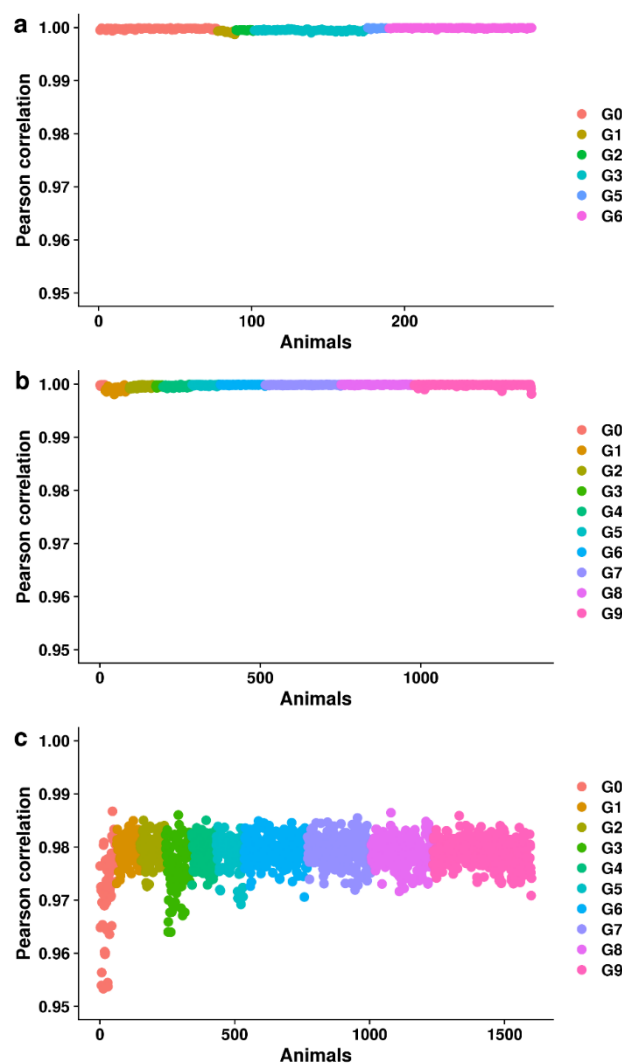
256 **Results**

257 **Genotype quality control and imputation**

258 True SNPs genotyping data were available for all sires and dams from G0 to G9. The quality
259 control of the genotypes was first carried out for each SNP chip independently. With a CR
260 threshold of 90%, 10 animals genotyped with the 70k SNPs chip and no individual genotyped
261 with the 60K and 650K SNPs chips were discarded (Additional file 1). For the SNPs, 15,114
262 SNPs from the 60K SNPs chip (5,776 for $CF < 95\%$ and 9,125 for $MAF < 1\%$), 11,891 SNPs
263 from the 70K SNPs chip (5,323 for $CF < 95\%$ and 6,568 for $MAF < 1\%$), and 99,587 SNPs
264 from the HD SNPs chip (53,735 for $CF < 95\%$ and 45,852 for $MAF < 1\%$) were removed. In
265 total, genotypes of 286 animals for 49,118 SNPs for the 60k SNPs chip, genotypes for 1,346
266 animals for 56,625 SNPs for the 70K SNPs chip, and finally genotypes for 32 animals for
267 559,105 SNPs for the HD SNPs chip were retained for further analyses (Additional file 2).

268 To obtain HD genotypes for all parents of the design, two successive runs of imputations
269 were performed. First, the imputation of the missing genotypes on each MD support (60K and
270 70K SNPs chips) allowed obtaining genotypes for 66,988 SNPs for all sires and dams. The

271 imputation accuracy was on average 0.995 regardless the generation of the imputed individuals
272 (Figures 1a and 1b). A second run of imputation was applied to all breeding animals from the
273 32 founder individuals genotyped with the HD SNPs chip. The imputation accuracy was also
274 high, with average accuracies around 0.979 (Figure 1c). Some few animals in G0 and G3 had
275 accuracies lower than 0.97. The accuracy estimated via the leave-one-out approach confirmed
276 the values estimated with the correlations, with an average of 0.975. In total, genotypes for
277 570,447 SNPs were obtained for all parents from G0 to G9.



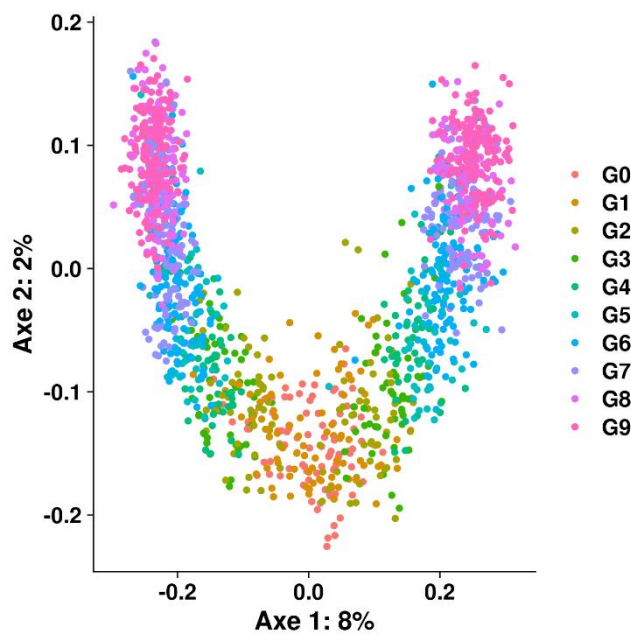
278

279 **Figure 1 Correlations between true and imputed genotypes for animals genotyped on 60K or 70K**
280 **SNPs chip.** For each analysis, correlations were estimated setting 5,000 SNPs as missing (5 batches of
281 1,000 SNPs) on one chip among SNPs in common between the two supports used. Animals are sorted
282 and colored by generation. Correlations between true and imputed genotypes (a) for the 286 animals
283 genotyped with the 60K SNPs chip using animals with 70K genotypes as reference population, and (b)

284 for the 1,346 animals genotyped with the 70K SNPs chip using animals with 60K genotypes as reference.
285 (c) Correlations between true and imputed genotypes after imputation to 650K SNPs from the imputed
286 medium density genotypes.

287

288 An MDS analysis was performed on the genotypic matrix to represent the changes of
289 genomic content of the lines with generations (Figure 2). The first component corresponded to
290 the dispersion of individuals according to the lines, and the second component corresponded to
291 the successive generations in both lines.



292

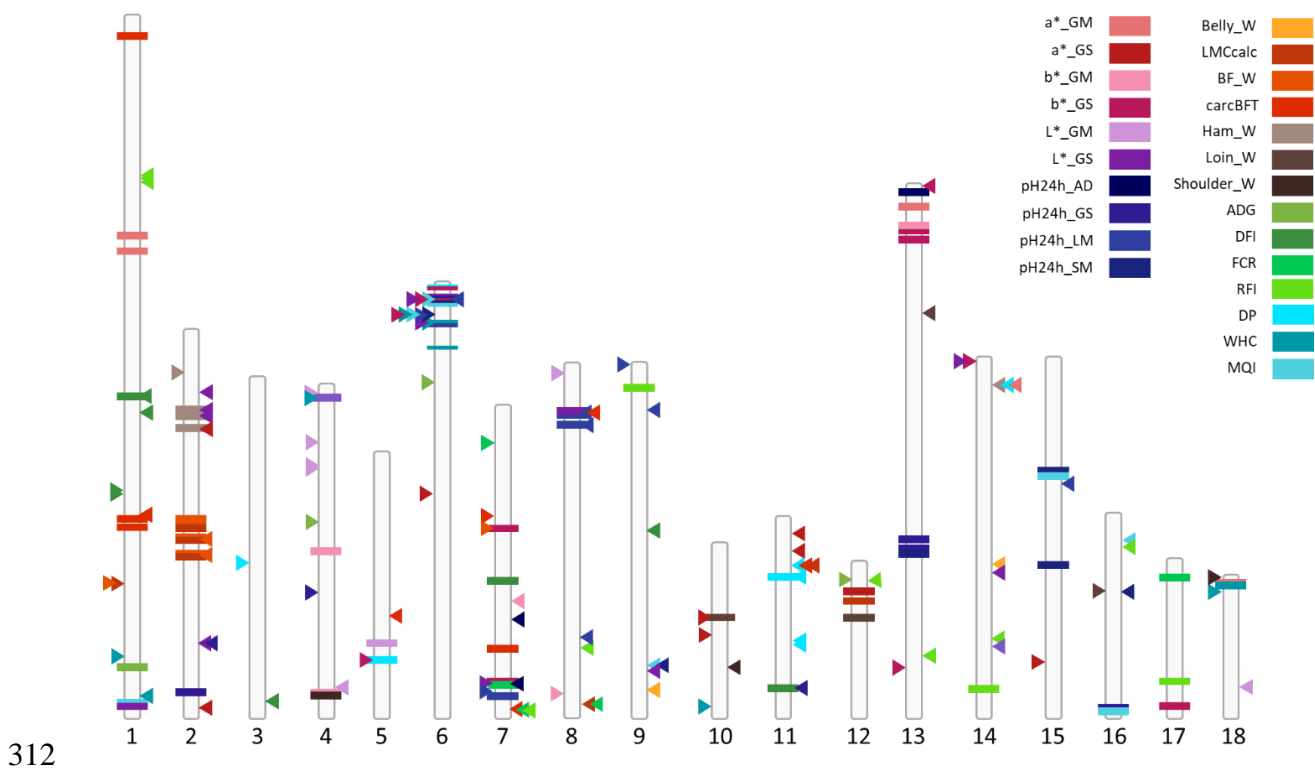
293 **Figure 2** Two first axes of the multidimensional scaling (MDS) analysis, based on the 570,447
294 **genotypes**. Points represent individuals (corresponding to all sires and dams of the population, N=1,632)
295 and colors are generations.

296

297 **Genome-wide association studies**

298 From the imputed genotypes of all parents, an average genotype was computed for all response
299 animals. Thus genotypes coded 0, 0.5, 1, 1.5 or 2 were available for 2,426 individuals in total.
300 Within a sibling, all individuals shared the same average genotype. On average the size of the
301 siblings was 4.07 (\pm 2.9).

302 First, association studies corresponding to Global-GWAS were carried out on all
 303 response animals, for each of the 24 traits. A total of 54 regions of 1 Mb (38 regions), 2 Mb (12
 304 regions), or 3 Mb (4 regions) were significant for at least one trait, corresponding to 72 QTL
 305 (trait x region). QTL were detected for all 24 traits (Figure 3), the list and characteristics of
 306 these QTL is reported in the Additional file 3. Cut weights were the traits with the lower number
 307 of QTL (1 to 3 per analysis), except for the weight of backfat (BF_W) in the Global-GWAS
 308 (Table 1). Meat quality measurements had the highest number of QTL (up to 7). Thirty regions
 309 associated with growth, feed intake, and feed efficiency were detected, including 12 regions
 310 associated with RFI and 5 with FCR. For all traits (except Belly_W), at least one QTL was
 311 detected in the Global-GWAS.

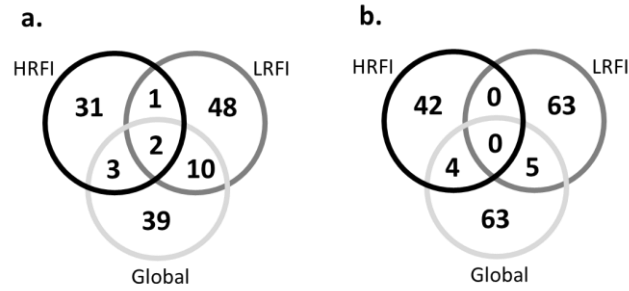


312
 313 **Figure 3 Location of all SNP-QTL identified on the 18 autosomes from the Global-GWAS, LRFI-**
 314 **GWAS and HRFI-GWAS.** The SNP-QTL corresponding to Global-GWAS are represented by
 315 horizontal bars, LRFI-GWAS by arrows to the right of the chromosomes and HRFI-GWAS by arrows
 316 to the left of the chromosomes. Each color represents one of the 24 traits
 317 *LRFI*: low RFI line, *HRFI*: high RFI line
 318 *DFI*: daily feed intake; *ADG*: average daily gain; *FCR*: feed conversion ratio; *RFI*: residual feed intake; *carcBFT*: backfat
 319 thickness measured on carcass; *a*_GM*: a* measured on the *gluteus medius* muscle; *a*_GS*: a* measured on the *gluteus*

320 *superficialis* muscle; *b*_GM*: *b** measured on the *gluteus medius* muscle; *b*_GS*: *b** measured on the *gluteus superficialis*
321 muscle; *L*_GM*: *L** measured on the *gluteus medius* muscle; *L*_GS*: *L** measured on the *gluteus superficialis* muscle;
322 *pH24h_AD*: pH 24h after slaughter measured on the adductor femoris muscle; *pH24h_GS*: pH 24h after slaughter measured
323 on the *gluteus superficialis* muscle; *pH24h_LM*: pH 24h after slaughter measured on the *longissimus dorsi* muscle; *pH24h_SM*:
324 pH 24h after slaughter measured on the *semimembranosus* muscle; *WHC*: water holding capacity of the *gluteus superficialis*
325 muscle; *MQI*: meat quality index; *LMCalc*: lean meat content of the carcass; *DP*: carcass dressing percentage; *Belly_W*: belly
326 weight; *BF_W*: backfat weight; *Ham_W*: ham weight; *Loin_W*: loin weight; *Shoulder_W*: shoulder weight
327

328 To assess whether the identified QTL regions were identical and shared in the two lines,
329 complementary GWAS analyses were performed per line, using either the set of individuals
330 from G1 to G9 of the HRFI line or the set of individuals from G1 to G9 of the LRFI line. For
331 analyses performed by line, the number of regions detected for a trait could differ between lines.
332 For instance, more loci were detected in the HRFI line for *b*_GS*, *L*_GM* and *WHC*, whilst
333 more regions were detected in the LRFI line for *RFI*, *carcBFT*, *DP*, *pH24h_LM* and
334 *pH24h_AD*. In the HRFI line, 46 QTL were identified in 37 regions, and in the LRFI line, 68
335 QTL were identified in 61 regions. Only 3 regions overlapped in the two lines: on SSC6, a
336 region located between 7 to 10 Mb affected *pH24h_LM* in LRFI and *L*_GS*, *b*_GS*, and *MQI*
337 in HRFI, on SSC7, a region from 107 to 109 Mb affected *L*_GS* in HRFI and *pH24h_AD* in
338 LRFI, and on SSC12, a region located between 7 to 9 Mb affected *ADG* in HRFI and *RFI* in
339 LRFI. The two first regions affected highly correlated traits related to meat quality, but the last
340 region affected uncorrelated traits.

341 Fifteen regions were shared between the 54 regions identified in the Global-GWAS and
342 the 95 unique regions from the analyses per line, with only 3 regions common to the Global-
343 GWAS and HRFI-GWAS analyses, 10 common to Global-GWAS and LRFI-GWAS, and the
344 SSC6 and SSC7 regions described above detected in the three analyses (Figure 4a). Among
345 these regions only 9 QTL (trait x region) were identified jointly in the Global-GWAS and in
346 one of the Lines-GWAS (Figure 4b), and none was shared in the three analyses.

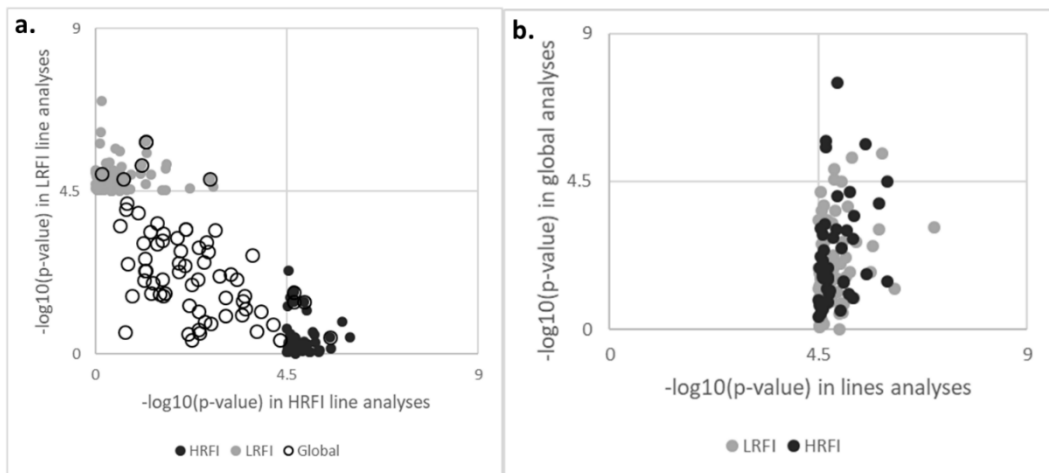


347

348 **Figure 4 Comparison of GWAS results obtained from Global-GWAS (Global), HRFI-GWAS**
349 **(HRFI) and LRFI-GWAS (LRFI).** Comparison of the number of identical regions (a) and (b)
350 comparison of the number of identical QTL (trait x region)

351

352 Very few QTL were thus common to the three GWAS (Figure 3). To assess whether a SNP-
353 QTL significant in one analysis reached significance or suggestive thresholds in the other
354 analyses, their p -values were compared. First, comparing the Lines-GWAS (Figure 5a), SNP-
355 QTL detected *via* HRFI-GWAS had $-\log_{10}(p\text{-values})$ generally lower than 1 in the LRFI-
356 GWAS, and none reached the suggestive threshold of 3. Similar results were obtained
357 comparing SNP-QTL of the LRFI-GWAS to their p -values with the HRFI-GWAS. For the
358 SNP-QTL significant in the Global-GWAS, the $-\log_{10}(p\text{-values})$ with the Lines-GWAS were
359 intermediate and exceeded the suggestive threshold for several QTL. It should be noted that for
360 these SNP-QTL, when the $-\log_{10}(p\text{-values})$ was suggestive in one line, it was lower in the other
361 line.



362

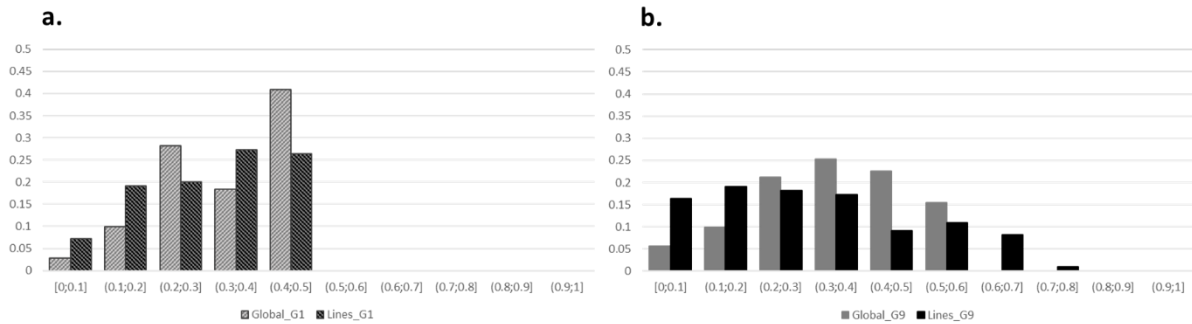
363 **Figure 5 Plot of the $-\log_{10}(p\text{-value})$ of the SNP-QTL.** The $-\log_{10}(p\text{-value})$ are obtained in first case
364 with the two lines analyses for all SNP-QTL detected for the lines or the global analyses (a), and in
365 second case obtained with the global analysis for SNP-QTL detected with the GWAS performed per
366 line (b).

367

368 In addition, for the SNP-QTL corresponding to the QTL detected in the line analyses
369 (HRFI-GWAS and LRFI-GWAS), the $-\log_{10}(p\text{-values})$ obtained in the Global-GWAS were also
370 low (Figure 5b), with three-quarters (74.5%) of the SNP-QTL having $-\log_{10}(p\text{-values})$ lower
371 than 3.

372 **Change of allele frequencies over the generations**

373 The allele frequencies of the SNP-QTL detected either in Global-GWAS or in Lines-GWAS
374 were evaluated in G1 to G9 to reflect the informativeness of these GWAS (called G9 hereafter)
375 and in G1. When the SNP-QTL was detected in the Global-GWAS, all response animals were
376 used to compute the frequencies; for SNP-QTL from the Lines-GWAS only the animals of the
377 significant analysis (HRFI-GWAS or LRFI-GWAS) were used. The resulting frequency
378 histograms are shown in Figure 6. With G1 only, 87% of the SNP-QTL of the Global-GWAS
379 had an allele frequency between 0.2 and 0.5, with half of them between 0.4 and 0.5. In addition,
380 28% of SNP-QTL of the Lines-GWAS have a frequency <0.2 in G1 (Figure 6a), so the
381 distribution of the allele frequencies of the SNP-QTL between low (<0.2) and medium was
382 significantly different between the types of analyses ($P < 0.02$ for a Chi^2 with 1 df). This
383 difference in the distribution of the SNP-QTL allele frequencies between the two types of
384 analyses was preserved in G9 (Figure 6b, $P < 0.005$): 16% of the SNP-QTL of the Global-
385 GWAS had a frequency <0.2 , compared to 35% for the SNP-QTL of the Lines-GWAS. In
386 addition, 9% of the SNP-QTL of the Lines-GWAS had a frequency >0.6 , no marker reached
387 this frequency among SNP-QTL of the Global-GWAS.

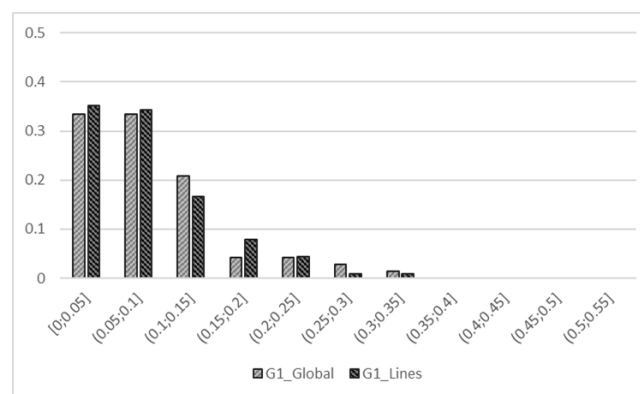


388

389 **Figure 6 Distribution of SNP-QTL allele frequencies of Global-GWAS (in grey) and Lines-GWAS**
 390 **(in black).** Distribution representing individuals from the line of the significant analysis (a) in G1
 391 generation (G1 individuals only) and (b) in G9 generation (G1 to G9 individuals).

392

393 In addition to the estimation of the global allelic frequencies, we controlled if in each line the
 394 detected SNP-QTL evolved differently according to the type of analysis. First, the differences
 395 of allele frequency differences between the HRFI and LRFI lines were estimated in the G1
 396 generation (at the beginning of the selection) (Figure 7). Regardless the analysis in which the
 397 SNP-QTL was detected, more than 65% of the SNP-QTL had low line frequency differences
 398 (<0.1) and less than 10% of the SNP-QTL had a line frequency difference >0.2. These SNP-
 399 QTL were not particularly found in one or the other type of analysis, in both types of analyses.



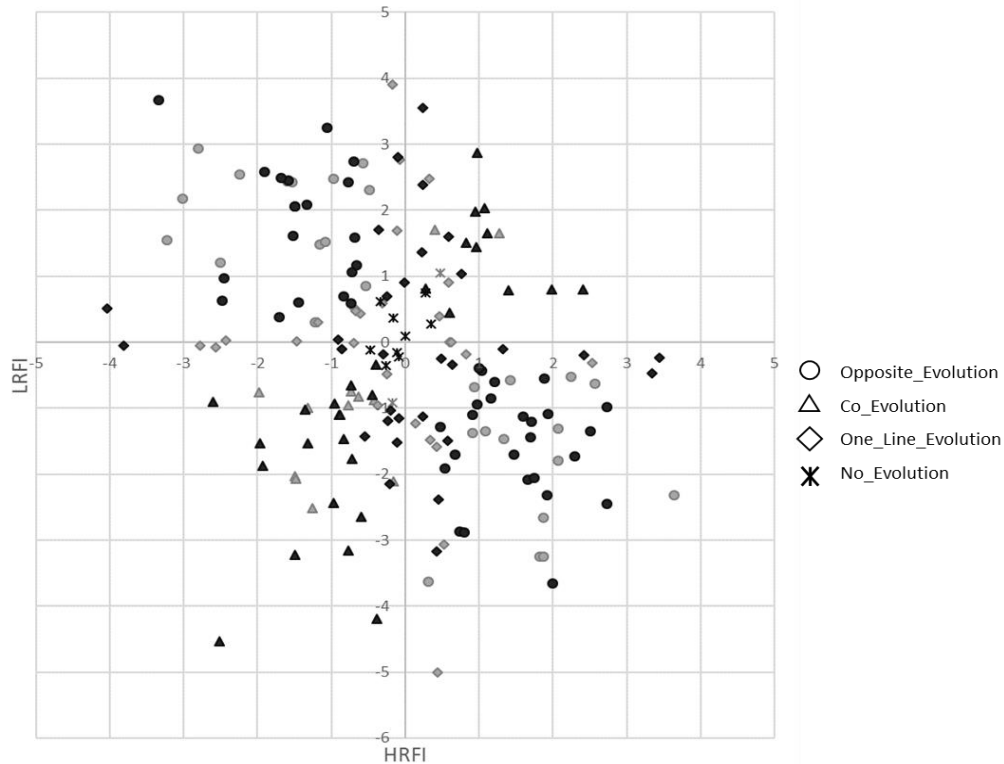
400

401 **Figure 7 Distribution of allele frequency differences between the lines.** The allele frequency
 402 differences are the absolute values between lines for SNP-QTL resulting from the Global-GWAS and
 403 Lines-GWAS in G1.

404

405 To better describe the changes of allele frequency over the generations, frequencies of SNP-
406 QTL from Global-GWAS and Lines-GWAS were then successively estimated in each line by
407 adding data from the next generation to the previous generations: G1 allele frequencies were
408 obtained from G1 individuals alone, G2 allele frequencies were obtained from G1 and G2
409 individuals etc. Using the 9 resulting frequencies computed in each line, a linear regression of
410 the generation number on the allele frequencies was applied within line. The comparison
411 between lines of the regression coefficients of the allelic frequencies highlighted 4 distinct cases
412 (Figure 8): (1) markers whose frequencies did not change with line selection (slope did not
413 differ from zero Wald test, 5.9%), (2) markers co-selected in the two lines (slopes differed from
414 zero and had identical sign: 22.6%), (3) markers selected in opposite directions in the lines
415 (slopes differed from zero with different signs: 40.3%), and (4) markers whose frequencies
416 changed only in one line (slope different from zero in one line only, 16.7% in LRFI, 14.5% in
417 HRFI). Again no difference in the mean allele frequency evolution was observed for SNP-QTL
418 detected in one or the other type of analysis whatever the situation (p -value=0.87 (No-
419 evolution), 0.73 (Co-evolution), 0.50 (Opposite-evolution and 0.70 (One_Line_evolution) for
420 Student T test on the values of the slopes).

421



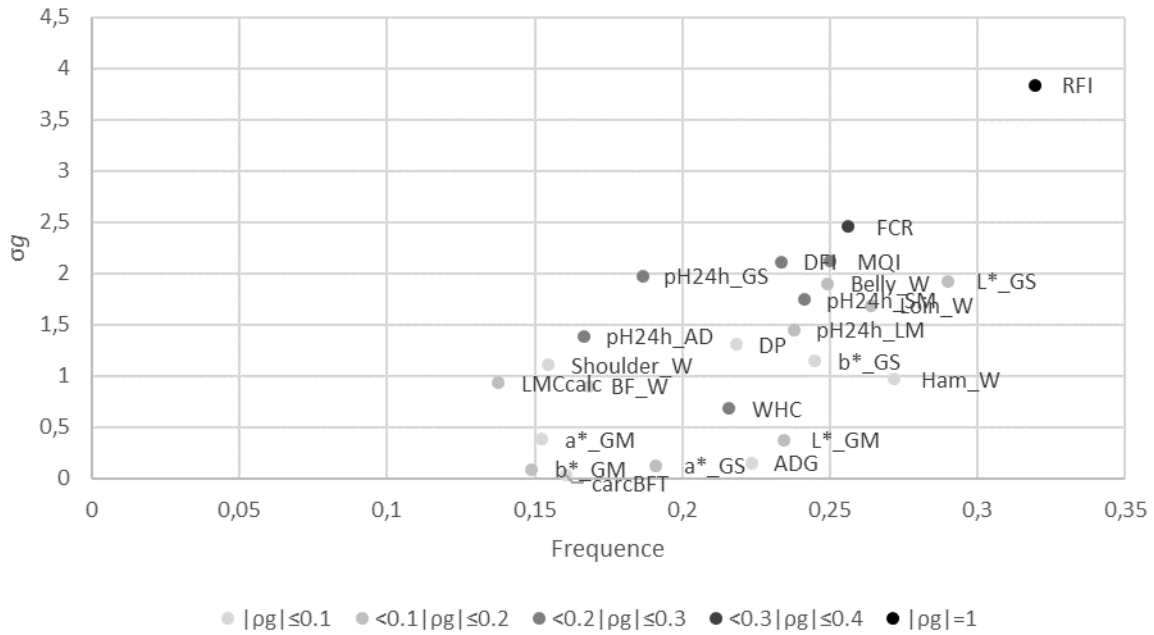
422

423 **Figure 8 Slopes of the linear regression equations of the allele frequencies on the 9 generations.**

424 Slopes were calculated in each line, for all SNP-QTL identified with Global-GWAS (in grey) and Lines-
425 GWAS (in black). Four situations (differentiated by different labels) were identified according to the
426 significance of the slope (different from zero with $p < 0.05$ with a Wald test) in one or the two lines.

427

428 For RFI in the two lines, 9 out of the 12 detected QTL corresponded to regions identified
429 with strong line frequencies differences: 3 RFI SNP-QTL showed differences in allelic
430 frequency between lines higher than 0.2 in G1. The other 6 RFI SNP-QTL showed large
431 changes of allelic frequency (regression slope > 0.024 /generation). To summarize the changes
432 of SNP-QTL allele frequencies for each trait, an average evolution score between G1 and G9
433 was computed using the estimated evolution scores of the different SNP-QTL detected for each
434 trait. These averages were between 0.11 (LMCcalc) and 0.24 (RFI). A correlation coefficient
435 of 0.66 was then estimated between the genetic line differences in G9 computed previously for
436 the 24 different traits [27] and these averages (Figure 9).



437

438 **Figure 9 Genetic differences in G9 between the two lines.** The genetic differences were expressed in
 439 genetic standard deviation of the trait (σ_g) as a function of the average evolution of allelic frequencies
 440 in the QTL regions of the trait between the two lines. The magnitude of the genetic correlation between
 441 each trait and RFI is indicated with a grey gradient.

442 *DFI*: daily feed intake; *ADG*: average daily gain; *FCR*: feed conversion ratio; *RFI*: residual feed intake;
 443 *carcBFT*: backfat thickness measured on carcass; *a*_GM*: a* measured on the *gluteus medius* muscle;
 444 *a*_GS*: a* measured on the *gluteus superficialis* muscle; *b*_GM*: b* measured on the *gluteus medius*
 445 muscle; *b*_GS*: b* measured on the *gluteus superficialis* muscle; *L*_GM*: L* measured on the *gluteus*
 446 *medius* muscle; *L*_GS*: L* measured on the *gluteus superficialis* muscle; *pH24h_AD*: pH 24h after
 447 slaughter measured on the adductor femoris muscle; *pH24h_GS*: pH 24h after slaughter measured on
 448 the *gluteus superficialis* muscle; *pH24h_LM*: pH 24h after slaughter measured on the *longissimus dorsi*
 449 muscle; *pH24h_SM*: pH 24h after slaughter measured on the *semimembranosus* muscle; *WHC*: water
 450 holding capacity of the *gluteus superficialis* muscle; *MQI*: meat quality index; *LMCcalc*: lean meat
 451 content of the carcass; *DP*: carcass dressing percentage; *Belly_W*: belly weight; *BF_W*: backfat weight;
 452 *Ham_W*: ham weight; *Loin_W*: loin weight; *Shoulder_W*: shoulder weight

453

454 Discussion

455 The objective of this study was to identify QTL affecting RFI and production traits in pig lines
 456 divergently selected for RFI and to understand if the traits had different genetic backgrounds
 457 between the lines. By optimizing the genotyping to reach a good power to detect QTL in the

458 full design and in the two lines separately, QTL were detected for all traits and hypotheses about
459 the trait genetic background in the two lines can be formulated.

460 **Using average parental genotypes to detect QTL**

461 While the use of SNPs chips now enables the genotyping of an individual at a reasonable cost,
462 the genotyping of a design comprising several thousand individuals represents nevertheless a
463 significant investment. In each generation of our design, at least two parities were produced,
464 one aiming at selecting future breeders, and one to control the responses to the selection on feed
465 consumption, growth and meat quality traits via measurements at the slaughterhouse. After 9
466 generations of selection, around 2,500 "response animals" had phenotypes. These individuals
467 have the advantage of having individual records for unmeasured traits in breeders (post-mortem
468 measurements). To optimize the costs, we genotyped all 1,632 breeders with MD SNPs chips
469 to exhaustively survey the segregating alleles in the design. In addition, the 32 main contributors
470 to the design were chosen from the G0 sires and dams to be genotyped using the HD SNPs chip,
471 and an imputation step was carried out to have HD genotypes for all breeding individuals. The
472 strong pedigree relationships in the design enabled a very good quality of HD imputation, as
473 they help to better detect long haplotypes used to infer missing SNPs [28]. A second step was
474 carried out, so that each response non-genotyped animal could have a genotype. These non-
475 genotyped animal imputation have been used in cattle [29] as part of genomic evaluations to
476 increase the size of the reference populations. In cattle, the most common situation is to
477 determine by imputation the genotypes of dams of bulls, knowing the genotypes of the maternal
478 grandsire, one (or more) offspring and the sires with which they were mated [30]. In such cases,
479 the strategy takes advantage of the family information (Mendelian rule of allele transmission)
480 and combined with allele frequencies and LD between markers at the population level. In our
481 case, at each generation n , all response animals had both parents genotyped at generation $n-1$.
482 Given these trio structures, an expected genotype at each position could be deduced from the

483 genotypes of the parents using simple segregation rules: since the genotypes were coded as an
484 allelic dosage for one reference allele, the genotype expectation for each offspring was simply
485 the average of the genotypes of its two parents. As a result, 2,426 animals with genotypes
486 (predicted) and phenotypes were available for subsequent GWAS analyses.

487 **Understanding the differences of detected regions between analyses**

488 The regions detected with each type of analysis (Global- or Lines-GWAS) were very different
489 and only 9 QTL out of 177 were shared between Global-GWAS and Lines-GWAS. The SNP-
490 QTL detected with the Global-GWAS were far from reaching the threshold of significance in
491 the Lines-GWAS. Similarly, most SNP-QTL detected with the Lines-GWAS were far from
492 reaching the threshold of significance in the Global-GWAS. Although the number of
493 individuals included in the Global-GWAS was twice higher than in the line analyses, the
494 addition of individuals belonging to the other line seemed to have reduced the power of
495 detection of QTL segregating in the first line. The SNP-QTL detected in the Global-GWAS or
496 Lines-GWAS differed for their allelic frequencies in G1. This difference remained at the whole
497 line level (G9): more SNPs with low allele frequencies were identified with the Lines-GWAS.
498 The pedigree kinship matrix was used in the GWAS model to correct for the strong genomic
499 structure of the population. If successful to control the type-I error of the analyses, this classical
500 approach also limits the power of detection of QTL in highly differentiated regions between
501 lines, as their link with the trait variability would be absorbed into the additive genetic
502 component of the model. The Global-GWAS thus essentially allow the detection of regions
503 segregating at intermediate frequencies in both lines. As an alternative, the analyses carried out
504 by line allow detecting regions that got close to fixation with selection in one of the lines. From
505 these results, it seems that the power of detection related to allele frequencies in each line is the
506 main difference between QTL-SNPs detected with the Lines-GWAS and Global-GWAS. Given
507 the power of the design, it is thus likely that the biological pathways involved in RFI variability

508 in the two lines are similar, but with different contributions to the trait in each line, contrary to
509 some previous hypotheses [10, 27].

510 **Comparison with published regions**

511 Among the 12 QTL detected for RFI, three regions are detected close to RFI QTL already
512 published. The region on SSC14 at 130-131 Mb is close to the region described by Duy N. Do
513 et al. [31] who proposed G-protein-coupled receptor kinase 5 (*GRK5*) (129,114,449-
514 129,343,412) as a candidate gene. Wang & al. [32] reported that a *GRK5* deficiency led to
515 insulin resistance and hepatic steatosis, and to decreases diet-induced obesity and adipogenesis
516 in mice. In position 131,181,710-131,579,703 *FGFR2* (fibroblast growth factor receptor 2)
517 could also be an interesting candidate. All four FGF receptors and several FGF ligands are
518 present in the intestine and are key players in controlling cell proliferation, differentiation,
519 epithelial cell restitution, and stem cell maintenance. *FGFR2* is expressed in the human ileum
520 and throughout adult mouse intestine [33]. The second region closest to published RFI QTL is
521 the 184-486 Mb interval on SSC13 near QTL reported by Bai et al. [34] and Duy N. Do et al.
522 [31]. In this region *TMPRSS15* (transmembrane serine protease 15) is an interesting candidate
523 gene. This gene encodes an intestinal enzyme responsible for initiating activation of pancreatic
524 proteolytic proenzymes. It catalyzes the conversion of trypsinogen to trypsin, which in turn
525 activates other proenzymes including chymotrypsinogen procarboxypeptidases and
526 proelastases. *TMPRSS15* has been associated to Enterokinase Deficiency, a life-threatening
527 intestinal malabsorption disorder characterized by diarrhea and failure to thrive [35]. On SSC17
528 two RFI QTL have been published by Duy N. Do et al. [31] close to the *SOGAI* gene
529 (suppressor of glucose, autophagy-associated protein 1, 40,020,107-40,098,992) and by Onteru
530 et al. [10] close to the *DOK5* gene (docking protein 5, 55,391,074-55,541,561). These two QTL
531 surround the region we detected and could correspond to one unique QTL. In position
532 48,090,077-48,100,816, and in position 48,132,911-48,149,732, respectively, *PLTP* and

533 *ZNF335* genes are additional candidate genes. In human, Coleman et al. [36] identified the
534 region encoding *ZNF335* as a susceptibility locus for the coeliac disease, a chronic immune-
535 mediated disease triggered by the ingestion of gluten [36]. The PLTP (phospholipid transfer
536 protein) transfers phospholipids from triglyceride-rich lipoproteins to high density lipoprotein
537 (HDL). In addition to regulating the size of HDL particles, this protein may be involved in the
538 cholesterol metabolism. PLTP KO mice absorb less cholesterol than WT mice, and have also
539 deficient secretion by the intestine [37].

540 **Potential pleiotropic effects**

541 The large number of traits recorded in our design and the known genetic correlations between
542 these traits [27] enable the detection of pleiotropic regions, i.e. regions affecting multiple traits.
543 Among the five regions detected for FCR, only the QTL located between 117 Mb and 119 Mb
544 on SSC7 co-localized with a RFI QTL. For the other traits correlated to RFI (DFI, MQI, WHC,
545 pH24h_AD, pH24h_GS, and pH24h_SM traits), only 3 QTL were detected within 10 Mb of
546 the RFI QTL: a QTL at 2 Mb influencing MQI on SSC16 between 11 and 12 Mb, and two QTL
547 on pH24h_AD at 7 Mb and 10 Mb of QTL for RFI located at 113-114 Mb on SSC14 and 107-
548 109 Mb on SSC7, respectively. Compared to the previously published QTL regions for RFI,
549 we identified a QTL influencing FCR in a region described by Onteru et al. [10] between 15
550 and 16 Mb on SSC7, a QTL for pH24h_SM in the 80 and 81Mb interval on SSC15 described
551 by Duy N Do et al. [31], and a QTL for DFI in the region described by Y M Guo et al. [38] on
552 SSC3 between positions 126 and 128Mb. Despite the reported correlations between these traits
553 and RFI, among the 52 QTL detected in our study for DFI, MQI, WHC, pH24h_AD,
554 pH24h_GS, and pH24h_SM, only seven co-located with RFI QTL identified in our study or in
555 previously published studies.

556 **Changes of QTL allele frequencies and trait responses to selection**

557 The allele frequencies of the majority of the detected regions changed between the G1 and G9
558 generations, with more than 70% of the regions for which SNP-QTL evolved in opposite
559 directions or in a one line only. However, the magnitude of allelic changes of the QTL regions
560 varied from one trait to the next, and was strongly correlated with line differences previously
561 reported in G9 [27]. Indeed, the regions with the highest allele frequency changes were detected
562 for RFI, which was trait used for selection. For the other traits, the higher the genetic correlation
563 with RFI, the higher the frequency variation of the associated QTL regions. As a result, QTL
564 affecting FCR, DFI and MQI had the highest frequency changes with generations. The
565 responses of QTL affecting meat quality traits are consistent with the high and early responses
566 to selection previously detected in this experimental population for these traits [5]. Altogether,
567 our analyses underline a clear relationship between the quantitative responses to selection of
568 the traits and changes of alleles frequencies in some QTL regions, certainly pointing out
569 chromosomic regions that were selected during the experiment, whereas in such populations of
570 low effective size and strong directional selection, detecting selection signatures with standard
571 methodologies [39] can have low power due to the major effect of drift on the changes of the
572 allele frequencies. However, recently developed new methods, based on genetic time series
573 could provide new insights for the detection of regions under selection in small populations
574 [40].

575 **Conclusions**

576 This study aimed at characterizing the molecular architecture of RFI in two lines divergently
577 selected for this trait. Besides efficiently detecting known and new QTL regions, the
578 combination of GWAS carried out per line or simultaneously using all individuals allowed the
579 identification of candidate regions of the genome under selection, which can explain the
580 responses to selection of different traits reported before. Analyzing the allelic frequencies from
581 G1 to G9, we concluded that the majority of the QTL regions responded to selection in a

582 divergent way in the lines, and that the same metabolic pathways were certainly involved in
583 both lines. Several new regions determining RFI variability were identified in this study and
584 new candidate genes were proposed to complement the data acquired in previous published
585 analyses.

586 **Declarations**

587 **Ethics approval and consent to participate**

588 All pigs were reared in compliance with national regulations and according to procedures
589 approved by the French Veterinary Services at INRA experimental facilities. The care and use
590 of pigs were performed following the guidelines edited by the French Ministries of High
591 Education, Research and Innovation, and of Agriculture and Food
592 (<http://ethique.ipbs.fr/sdv/charteexpeanimale.pdf>).

593 **Consent for publication**

594 Not applicable

595 **Availability of data and materials**

596 The datasets used and/or analysed during the current study are available from the corresponding
597 author on reasonable request.

598 **Competing interests**

599 The authors declare that they have no competing interests.

600 **Funding**

601 This study and the two first authors were financially supported by the French National Research
602 Agency via the PIG_FEED and MicroFeed projects, under grants ANR-08-GENM-038 and
603 ANR-16-CE20-0003.

604 **Authors' contributions**

605 ED performed the statistical analyses and wrote the first draft of the paper. YB and KF
606 organized the data acquisition. ED and YL performed the imputation and quality control of the

607 genotypic data. ED, AA, YL, HG and JR participated in the design of the study. JR and HG
608 provided scientific supervision. All authors read and approved the final manuscript.

609 **Acknowledgements**

610 The authors would like to thank (*i*) the experimental farm staff for data collection, samples
611 management and breeding of the animals and (*ii*) both technology platforms, CRCT and
612 Gentyane, for the genotyping.

613

614 **References**

- 615 1. McGlone J, Pond WG. Pig Production: Biological Principles and Applications. Cengage
616 Learning; 2003.
- 617 2. Soleimani T, Gilbert H. Evaluating environmental impacts of selection for residual feed
618 intake in pigs. *animal*. 2020;:1–11.
- 619 3. Webb AJ, King JWB. Selection for improved food conversion ratio on ad libitum group
620 feeding in pigs. *Animal Science*. 1983;37:375–85.
- 621 4. Koch RM, Swiger LA, Chambers D, Gregory KE. Efficiency of Feed Use in Beef Cattle. *J*
622 *Anim Sci*. 1963;22:486–94.
- 623 5. Gilbert H, Bidanel J-P, Gruand J, Caritez J-C, Billon Y, Guillouet P, et al. Genetic parameters
624 for residual feed intake in growing pigs, with emphasis on genetic relationships with carcass
625 and meat quality traits. *J Anim Sci*. 2007;85:3182–8.
- 626 6. Cai W, Casey DS, Dekkers JCM. Selection response and genetic parameters for residual feed
627 intake in Yorkshire swine. *J Anim Sci*. 2008;86:287–98.
- 628 7. Drouilhet L, Achard CS, Zemb O, Molette C, Gidenne T, Larzul C, et al. Direct and correlated
629 responses to selection in two lines of rabbits selected for feed efficiency under ad libitum and
630 restricted feeding: I. Production traits and gut microbiota characteristics. *J Anim Sci*.
631 2016;94:38–48.
- 632 8. Ramayo-Caldas Y, Ballester M, Sánchez JP, González-Rodríguez O, Revilla M, Reyer H, et
633 al. Integrative approach using liver and duodenum RNA - Seq data identifies candidate genes
634 and pathways associated with feed efficiency in pigs. *Scientific Reports*. 2018;8:558.
- 635 9. Messad F, Louveau I, Koffi B, Gilbert H, Gondret F. Investigation of muscle transcriptomes
636 using gradient boosting machine learning identifies molecular predictors of feed efficiency in
637 growing pigs. *BMC Genomics*. 2019;20:659.
- 638 10. Onteru SK, Gorbach DM, Young JM, Garrick DJ, Dekkers JCM, Rothschild MF. Whole
639 Genome Association Studies of Residual Feed Intake and Related Traits in the Pig. *PLOS ONE*.
640 2013;8:e61756.
- 641 11. Ding R, Yang M, Wang X, Quan J, Zhuang Z, Zhou S, et al. Genetic Architecture of Feeding
642 Behavior and Feed Efficiency in a Duroc Pig Population. *Front Genet*. 2018;9.
643 doi:10.3389/fgene.2018.00220.
- 644 12. Hu Z-L, Park CA, Reecy JM. Building a livestock genetic and genomic information
645 knowledgebase through integrative developments of Animal QTLdb and CorrDB. *Nucleic*
646 *Acids Res*. 2019;47:D701–10.
- 647 13. Sosa-Madrid BS, Santacreu MA, Blasco A, Fontanesi L, Pena RN, Ibáñez-Escriche N. A
648 genomewide association study in divergently selected lines in rabbits reveals novel genomic
649 regions associated with litter size traits. *Journal of Animal Breeding and Genetics*.
650 2020;137:123–38.

- 651 14. Daumas G. Taux de muscle des pièces et appréciation de la composition corporelle des
652 carcasses. :7.
- 653 15. Charpentier J, Monin G, Ollivier L. Correlations between carcass characteristics and meat
654 quality in Large White pigs. Proceedings of the 2nd International Symposium on Conditions
655 and Meat Quality of Pigs. 1971. [https://agris.fao.org/agris-](https://agris.fao.org/agris-search/search.do?recordID=US201302309831)
656 [search/search.do?recordID=US201302309831](https://agris.fao.org/agris-search/search.do?recordID=US201302309831). Accessed 5 Oct 2020.
- 657 16. Tribout T, Caritez J-C, Gogué J, Gruand J, Bouffaud M, Billon Y, et al. Estimation, par
658 utilisation de semence congelée, du progrès génétique réalisé en France entre 1977 et 1998 dans
659 la race porcine Large White : résultats pour quelques caractères de production et de qualité des
660 tissus gras et maigres. :8.
- 661 17. Noblet J, Karege C, Dubois S, van Milgen J. Metabolic utilization of energy and
662 maintenance requirements in growing pigs: effects of sex and genotype. *J Anim Sci*.
663 1999;77:1208–16.
- 664 18. Purcell S, Neale B, Todd-Brown K, Thomas L, Ferreira MAR, Bender D, et al. PLINK: A
665 Tool Set for Whole-Genome Association and Population-Based Linkage Analyses. *The*
666 *American Journal of Human Genetics*. 2007;81:559–75.
- 667 19. Warr A, Affara N, Aken B, Beiki H, Bickhart DM, Billis K, et al. An improved pig reference
668 genome sequence to enable pig genetics and genomics research. *Gigascience*. 2020;9.
669 doi:10.1093/gigascience/giaa051.
- 670 20. Sargolzaei M, Chesnais JP, Schenkel FS. A new approach for efficient genotype imputation
671 using information from relatives. *BMC Genomics*. 2014;15:478.
- 672 21. Purcell S, Neale B, Todd-Brown K, Thomas L, Ferreira MAR, Bender D, et al. PLINK: a
673 tool set for whole-genome association and population-based linkage analyses. *Am J Hum*
674 *Genet*. 2007;81:559–75.
- 675 22. Zhou X, Stephens M. Genome-wide efficient mixed-model analysis for association studies.
676 *Nat Genet*. 2012;44:821–4.
- 677 23. Aliakbari A, Delpuech E, Labrune Y, Riquet J, Gilbert H. The impact of training on data
678 from genetically-related lines on the accuracy of genomic predictions for feed efficiency traits
679 in pigs. *Genet Sel Evol*. 2020;52:57.
- 680 24. Zhou X, Carbonetto P, Stephens M. Polygenic Modeling with Bayesian Sparse Linear
681 Mixed Models. *PLOS Genetics*. 2013;9:e1003264.
- 682 25. Gao X. Multiple testing corrections for imputed SNPs. *Genetic Epidemiology*.
683 2011;35:154–8.
- 684 26. Korte A, Farlow A. The advantages and limitations of trait analysis with GWAS: a review.
685 *Plant Methods*. 2013;9:29.
- 686 27. Gilbert H, Billon Y, Brossard L, Faure J, Gatellier P, Gondret F, et al. Review: divergent
687 selection for residual feed intake in the growing pig. *animal*. 2017;11:1427–39.

- 688 28. Ullah E, Mall R, Abbas MM, Kunji K, Nato AQ, Bensmail H, et al. Comparison and
689 assessment of family- and population-based genotype imputation methods in large pedigrees.
690 *Genome Res.* 2019;29:125–34.
- 691 29. Bouwman AC, Hickey JM, Calus MP, Veerkamp RF. Imputation of non-genotyped
692 individuals based on genotyped relatives: assessing the imputation accuracy of a real case
693 scenario in dairy cattle. *Genet Sel Evol.* 2014;46:6.
- 694 30. Pimentel EC, Wensch-Dorendorf M, König S, Swalve HH. Enlarging a training set for
695 genomic selection by imputation of un-genotyped animals in populations of varying genetic
696 architecture. *Genetics Selection Evolution.* 2013;45:12.
- 697 31. Do DN, Ostersen T, Strathe AB, Mark T, Jensen J, Kadarmideen HN. Genome-wide
698 association and systems genetic analyses of residual feed intake, daily feed consumption,
699 backfat and weight gain in pigs. *BMC Genetics.* 2014;15:27.
- 700 32. Wang L, Shen M, Wang F, Ma L. GRK5 ablation contributes to insulin resistance.
701 *Biochemical and Biophysical Research Communications.* 2012;429:99–104.
- 702 33. Danopoulos S, Schlieve CR, Grikscheit TC, Alam DA. Fibroblast Growth Factors in the
703 Gastrointestinal Tract: Twists and Turns. *Developmental Dynamics.* 2017;246:344–52.
- 704 34. Bai C, Pan Y, Wang D, Cai F, Yan S, Zhao Z, et al. Genome-wide association analysis of
705 residual feed intake in Junmu No. 1 White pigs. *Animal Genetics.* 2017;48:686–90.
- 706 35. Holzinger A, Maier E, Bück C, Mayerhofer P, Kappler M, Haworth J, et al. Mutations in
707 the Proenteropeptidase gene are the molecular cause of congenital enteropeptidase deficiency.
708 2002. doi:10.1086/338456.
- 709 36. Coleman C, Quinn EM, Ryan AW, Conroy J, Trimble V, Mahmud N, et al. Common
710 polygenic variation in coeliac disease and confirmation of ZNF335 and NIFA as disease
711 susceptibility loci. *European Journal of Human Genetics.* 2016;24:291–7.
- 712 37. Liu Ruijie, Iqbal Jahangir, Yeang Calvin, Wang David Q.-H., Hussain M. Mahmood, Jiang
713 Xian-Cheng. Phospholipid Transfer Protein–Deficient Mice Absorb Less Cholesterol.
714 *Arteriosclerosis, Thrombosis, and Vascular Biology.* 2007;27:2014–21.
- 715 38. Guo YM, Zhang ZY, Ma JW, Ai HS, Ren J, Huang LS. A genomewide association study
716 of feed efficiency and feeding behaviors at two fattening stages in a White Duroc × Erhualian
717 F2 population. *J Anim Sci.* 2015;93:1481–9.
- 718 39. Fariello MI, Boitard S, Naya H, SanCristobal M, Servin B. Using haplotype differentiation
719 among hierarchically structured populations for the detection of selection signatures. *Genetics.*
720 2013;193:929–41.
- 721 40. Paris C, Servin B, Boitard S. Inference of Selection from Genetic Time Series Using
722 Various Parametric Approximations to the Wright-Fisher Model. *G3: Genes, Genomes,*
723 *Genetics.* 2019;9:4073–86.
- 724
- 725

726 **Table**

727 **Table 1 Number of QTL identified for each trait with the 3 groups of association studies**

Trait	Global	HRFI	LRFI	Total
DFI	3	2	4	9
ADG	1	3	0	4
FCR	2	1	2	5
RFI	3	0	9	12
carcBFT	4	1	5	10
a*_GM	4	0	1	5
a*_GS	1	4	4	9
b*_GM	3	1	1	5
b*_GS	7	5	1	13
L*_GM	1	5	2	8
L*_GS	3	4	6	13
pH24h_AD	2	0	3	5
pH24h_GS	5	1	2	8
pH24h_LM	4	3	6	13
pH24h_SM	4	1	2	7
WHC	3	6	1	10
MQI	4	2	2	8
LMCcalc	4	1	2	7
DP	3	1	7	11
Belly_W	0	0	2	2
BF_W	5	2	3	10
Ham_W	3	1	1	5
Loin_W	2	1	1	4
Shoulder_W	1	1	1	3
Total	59	39	48	186

728 Association studies on the full population (Global-GWAS, *Global*) and for each line separately (HRFI-
 729 GWAS, *HRFI* and LRFI-GWAS, *LRFI*) were performed. Traits with more than 3 QTL differences
 730 between the HRFI-GWAS and LRFI-GWAS analyses are highlighted in grey

731 *DFI*: daily feed intake; *ADG*: average daily gain; *FCR*: feed conversion ratio; *RFI*: residual feed intake;
 732 *carcBFT*: backfat thickness measured on carcass; *a*_GM*: a* measured on the *gluteus medius* muscle;
 733 *a*_GS*: a* measured on the *gluteus superficialis* muscle; *b*_GM*: b* measured on the *gluteus medius*
 734 muscle; *b*_GS*: b* measured on the *gluteus superficialis* muscle; *L*_GM*: L* measured on the *gluteus*
 735 *medius* muscle; *L*_GS*: L* measured on the *gluteus superficialis* muscle; *pH24h_AD*: pH 24h after
 736 slaughter measured on the adductor femoris muscle; *pH24h_GS*: pH 24h after slaughter measured on
 737 the *gluteus superficialis* muscle; *pH24h_LM*: pH 24h after slaughter measured on the *longissimus dorsi*

738 muscle; *pH24h_SM*: pH 24h after slaughter measured on the *semimembranosus* muscle; *WHC*: water
739 holding capacity of the *gluteus superficialis* muscle; *MQI*: meat quality index; *LMCcalc*: lean meat
740 content of the carcass; *DP*: carcass dressing percentage; *Belly_W*: belly weight; *BF_W*: backfat weight;
741 *Ham_W*: ham weight; *Loin_W*: loin weight; *Shoulder_W*: shoulder weight

742 **Additional files**

743 **Additional file 1**

744 Format: additionalfile1.xlsx

745 Title: Number of animals used for the analyses after quality control

746 Description: Details of the number of animals before and after application of filter on the call
747 rate (CR) were given for chips (60K, 70K and 650K SNPs chips), imputation levels (MD/HD
748 imputation) and average genotypes calculated from the genotypes of both parents (HD
749 predicted).

750

751 **Additional file 2**

752 Format: additionalfile2.xlsx

753 Title: Number of SNPs used for the analyses after quality control

754 Description: Details of the number of SNPs before and after application of filters on the call
755 frequency (CF) and the frequency of minor allele (MAF) were given for chips (60K, 70K and
756 650K SNPs chips), imputation levels (MD imputation and HD imputation) and average
757 genotypes calculated from the genotypes of both parents (HD predicted).

758

759 **Additional file 3**

760 Format: additionalfile3.xlsx

761 Title: QTL regions detected with the three groups of association studies

762 Description: These QTL regions were found from the full population (Global-GWAS) and from
763 each line separately (HRFI-GWAS and LRFI-GWAS)

764 *DFI*: daily feed intake; *ADG*: average daily gain; *FCR*: feed conversion ratio; *RFI*: residual feed intake; *carcBFT*:
765 backfat thickness measured on carcass; *a*_GM*: a* measured on the *gluteus medius* muscle; *a*_GS*: a* measured
766 on the *gluteus superficialis* muscle; *b*_GM*: b* measured on the *gluteus medius* muscle; *b*_GS*: b* measured on

767 the *gluteus superficialis* muscle; *L*_GM*: L* measured on the *gluteus medius* muscle; *L*_GS*: L* measured on
768 the *gluteus superficialis* muscle; *pH24h_AD*: pH 24h after slaughter measured on the adductor femoris muscle;
769 *pH24h_GS*: pH 24h after slaughter measured on the *gluteus superficialis* muscle; *pH24h_LM*: pH 24h after
770 slaughter measured on the *longissimus dorsi* muscle; *pH24h_SM*: pH 24h after slaughter measured on the
771 *semimembranosus* muscle; *WHC*: water holding capacity of the *gluteus superficialis* muscle; *MQI*: meat quality
772 index; *LMCalc*: lean meat content of the carcass; *DP*: carcass dressing percentage; *Belly_W*: belly weight;
773 *BF_W*: backfat weight; *Ham_W*: ham weight; *Loin_W*: loin weight; *Shoulder_W*: shoulder weight